

Conference Proceedings

2nd International Conference on Atmospheric Dust - DUST2016

PM source signature using simultaneous measurements of PM₁₀, PM_{2.5} and PM₁ chemical tracer concentrations

Antonio Speranza*, Rosa Caggiano, Salvatore Margiotta, Vito Summa, Serena Trippetta

IMAA, Istituto di Metodologie per l'Analisi Ambientale, CNR, Italy

**antonio.speranza@imaa.cnr.it*

Abstract

The study aims to identify the source signature of the particulate matter using the ratios between the chemical tracer (Tr) concentrations (i.e., Al, Ca, Cl, Fe, K, Mg, Na, NH⁴⁺, Ni, NO³⁻, Si, SO₄²⁻, Sr, Ti and V) content in PM₁₀, PM_{2.5} and PM₁ simultaneous measurements. Studies regarding the tracer concentrations of PM₁₀, PM_{2.5} and PM₁ were considered and the corresponding ratios (i.e. $PM_{1(Tr)}/PM_{10(Tr)}$, $PM_{2.5(Tr)}/PM_{10(Tr)}$ and $(PM_{2.5(Tr)}-PM_{1(Tr)})/(PM_{10(Tr)}-PM_{1(Tr)})$) were calculated and displayed using a dedicated triangular diagram. Results point out that the data relating to Al, Ca, Fe, Si, Sr and Ti (tracers mainly attributed to crustal sources) and to Cl, Mg and Na (tracers mainly related as sea-salt sources) are usually displayed towards the lower right region of the triangular diagram, where the tracer concentrations of the coarse size fraction are larger than the tracer concentrations of the fine and submicrometric size fractions. The data corresponding to Ni and V (tracers generally attributed to combustion sources) are displayed towards the upper region of the triangular diagram, where the tracer concentrations of the fine and submicrometric size fractions are larger than the tracer concentrations of the coarse size fraction. The tracer concentrations of the intermodal size fraction may not be negligible with respect to the tracer concentrations of coarse and submicrometric size fractions in this region. Finally, the data corresponding to tracers with more than one characteristic source, such as K (tracer interpreted as city dust and biomass burning) and SO⁴⁻ (tracer related to combustion sources, secondary aerosols and long-range transport combined with NH⁴⁺ and NO³⁻) may be displayed on different regions of the triangular diagram, depending on their different emission sources. Therefore, the triangular diagram can be useful for grouping tracers on the basis of their characteristic source signature.

Keywords: PM; Chemical tracers; Triangular diagram

1. Introduction

Air quality is currently a rising public and governmental concern because of detrimental health effects caused by pollutants and the resulting social-economical implications. Particulate matter (PM) is one of the pollutants affecting air quality with harmful effects on human health. Indeed, epidemiological studies have demonstrated that there are “lines that connect” exposure to fine particulate air pollution to cardiovascular and respiratory diseases (Pope and Dockery, 2006). Government institutions and international organizations have issued air quality standards and recommendations for the level of PM (European Directive 2008/50/EC), (WHO, 2006). However, in order to plan any action aiming to reduce PM for the protection of the environment and public health, it is mandatory to identify the possible emission sources of PM and their contribution to PM levels. A variety of methods were used to identify source apportionments and were reviewed by Viana et al. (2008) for the European contest. Receptor models are the most common approaches used, dealing with the measurements of the chemical composition of PM to the receptor sites. Further insight on the above techniques can be found in Belis et al. (2013).

The aim of this study is to identify the possible PM source signature. As such, chemical tracers determined in simultaneous measurements of different fractions of PM, as reported in literature, were considered and the corresponding ratios between tracer concentrations of size segregated PM were calculated and displayed using a dedicated triangular diagram.

2. Methodology

The triangular diagram (Speranza et al., 2014), (Speranza et al., 2016) was used to study the corresponding ratios between each tracer concentration of size segregated PM. The chemical tracers considered were Al, Ca, Cl, Fe, K, Mg, Na, NH_4^+ , Ni, NO_3^- , Si, SO_4^{2-} , Sr, Ti and V content in PM_{10} , $\text{PM}_{2.5}$ and PM_1 simultaneous measurements. The proposed approach is based on the evaluation of ratios between Tr concentrations of $\text{PM}_{2.5}$ and Tr concentration of PM_{10} (i.e. $\text{PM}_{2.5(\text{Tr})}/\text{PM}_{10(\text{Tr})}$ that is the contribution of fine fraction to PM_{10} of a specific tracer), and between Tr concentration of PM_1 and Tr concentration of PM_{10} (i.e. $\text{PM}_{1(\text{Tr})}/\text{PM}_{10(\text{Tr})}$ that is the contribution of submicron fraction to PM_{10} of a specific tracer). Furthermore, the triangular diagram shows the $(\text{PM}_{2.5(\text{Tr})} - \text{PM}_{1(\text{Tr})})/(\text{PM}_{10(\text{Tr})} - \text{PM}_{1(\text{Tr})})$ ratio which represents the proportion between the intermodal and the coarse size fraction of a specific tracer. Finally, the data is displayed by Graham and Midgley (2000).

3. Results and discussion

The triangular diagram shows that the ratios relating to the tracers, mainly representative of crustal sources and of African dust (i.e. Al, Ca, Fe, Mg, Si, Sr and Ti) and the ratios relating to tracers mainly from marine sources (i.e. Na, Cl and Mg) (Viana et al., 2008) Amato et al. (2009), Matassoni et al. (2011) and Visser et al. (2015) are mostly displayed toward the lower region of the triangular diagram. The tracer concentrations of the coarse size fraction are predominant.

The $\text{PM}_{2.5(\text{Tr})}/\text{PM}_{10(\text{Tr})}$ and $(\text{PM}_{2.5(\text{Tr})} - \text{PM}_{1(\text{Tr})})/(\text{PM}_{10(\text{Tr})} - \text{PM}_{1(\text{Tr})})$ ratios are below about 0.6, while $\text{PM}_{1(\text{Tr})}/\text{PM}_{10(\text{Tr})}$ ratios are below 0.4, see Fig.1-2. The calculated ratios relating to the tracers reported above show a characteristic grouping, a signature on the triangular diagram depending on the type of monitored site or specific pollution event. Indeed, the ratios for tracers relating to crustal sources for a rural site and for a kerbside site reported in Visser et al. (2015) are distinctly separate on the triangular diagram (see Fig.1). The

$PM_{2.5(Tr)}/PM_{10(Tr)}$ ratios range from about 0.24 to 0.36 for the kerbside site and from 0.36 to 0.52 for the rural site. The $PM_{1(Tr)}/PM_{10(Tr)}$ ratios range from about 0.05 to 0.11 for the kerbside site and from about 0.1 to 0.25 for the rural site. The $(PM_{2.5(Tr)}-PM_{1(Tr)})/(PM_{10(Tr)}-PM_{1(Tr)})$ ratios are between 0.2-0.46 for the two sites and are separated at about 0.3.

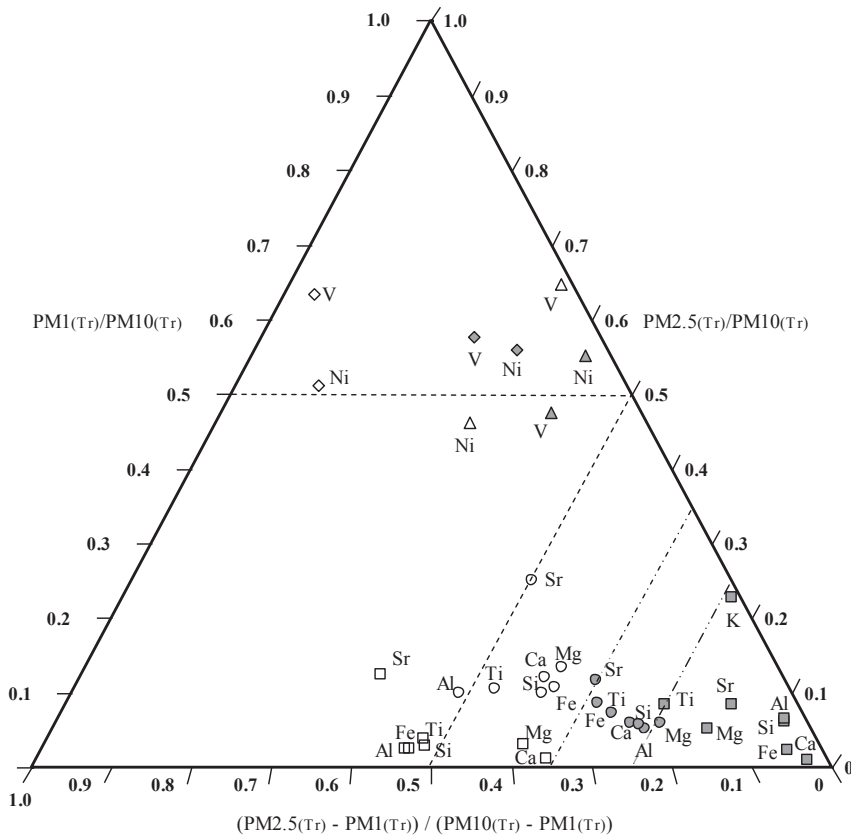


Fig. 1. Triangular diagram for tracer concentrations of PM_{10} , $PM_{2.5}$ and PM_1 of published data. Moreno et al. (2011) \diamond Summer \blacklozenge Winter - background site, \triangle Summer \blacktriangle Winter - regional background air monitoring station (rural site). Matassoni et al. (2011) \square in-dust days \blacksquare non-dust days -suburban background site. Visser et al. (2015) \square rural site \blacksquare kerbside site

Likewise, the calculated ratios for tracers related to crustal sources for a suburban background site with and without a Saharan dust outbreak (Matassoni et al., 2011) are well distinguishable on the triangular diagram. The $PM_{2.5(Tr)}/PM_{10(Tr)}$ ratios for non-dust days are plotted below 0.25, while the $PM_{2.5(Tr)}/PM_{10(Tr)}$ ratios for in-dust days are plotted between about 0.36 and 0.6. The $PM_{1(Tr)}/PM_{10(Tr)}$ ratios are just below 0.13 for both non-dust and in-dust conditions, while the $(PM_{2.5(Tr)}-PM_{1(Tr)})/(PM_{10(Tr)}-PM_{1(Tr)})$ ratios are separated by a wide gap from 0.2 to 0.36 (see Fig.1). Regarding the tracers mainly considered as marine sources, their ratios can also be distinguished clearly on the triangular diagram. The calculated ratios for an urban background site (Amato et al., 2009) are well separated from those reported for a background site (non-dust) (Matassoni et al., 2011) (see Fig. 2). The $PM_{2.5(Tr)}/PM_{10(Tr)}$ ratios are below 0.2 for Amato et al. (2009) and between 0.2 and 0.3 for

Matassoni et al. (2011). The $PM_{1(Tr)}/PM_{10(Tr)}$ and the $(PM_{2.5(Tr)}-PM_{1(Tr)})/(PM_{10(Tr)}-PM_{1(Tr)})$ ratios are contained for both sites below 0.1 and 0.3, respectively. The ratios of tracers related to the same source type such as crustal sources, desert dusts and sea-salt sources can therefore have similar proportions in each PM size fraction. Hence, they can be grouped on the triangular diagram and show characteristic source signatures.

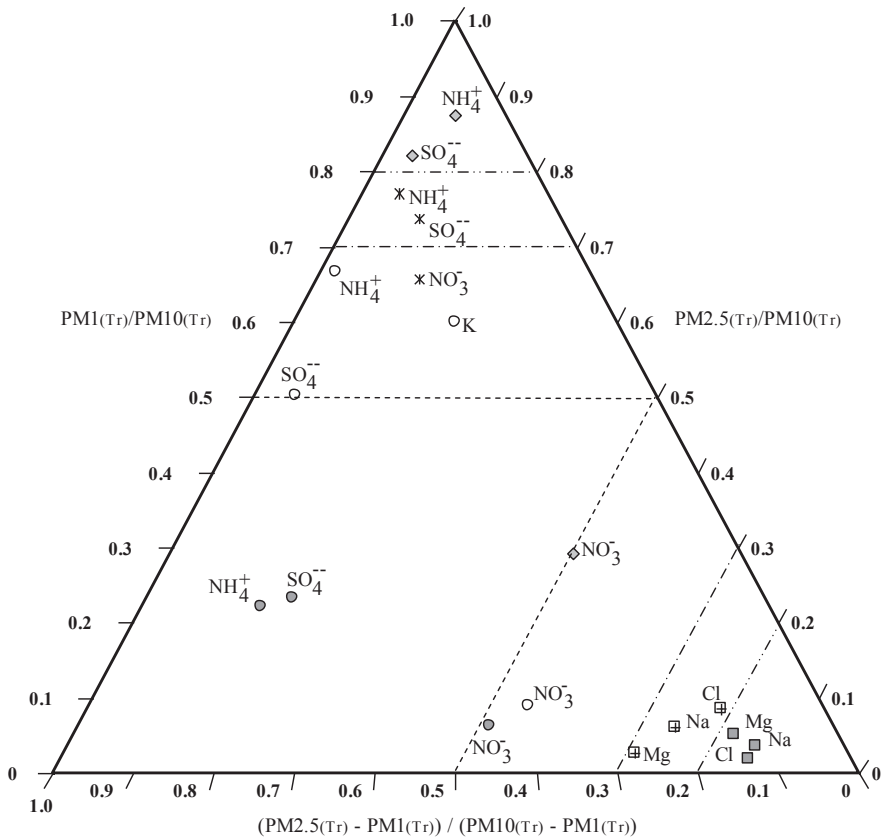


Fig. 2. Triangular diagram for tracer concentrations of PM_{10} , $PM_{2.5}$ and PM_1 of published data. Matassoni et al. (2011) \blacksquare non-dust days - suburban background site; Makkonen et al. (2010) \square Summer \blacksquare Winter - background site. Lim et al. (2012) \blacklozenge Asian outflows site. Rogula-Kozłowska et al. (2013) \ast urban background site. Amato et al. (2009) \boxplus urban background site

The triangular diagram shows that the ratios calculated for the tracers related to combustion sources (i.e. Ni, V) (Viana et al., 2008) Moreno et al. (2011) are mostly displayed toward the upper region of the triangular diagram where the tracer concentrations of fine and submicron size fractions are larger than the tracer concentrations of the coarser ones. The $PM_{2.5(Tr)}/PM_{10(Tr)}$ ratios are above 0.5 and the $PM_{1(Tr)}/PM_{10(Tr)}$ ratios are above 0.4, while the $(PM_{2.5(Tr)}-PM_{1(Tr)})/(PM_{10(Tr)}-PM_{1(Tr)})$ ratios show a wide variation between about 0.1 and 0.9 (see Fig.1). The calculated ratios related to tracers as Ni and V for an urban background and for a rural site are distinct on the triangular diagram (see Fig.1). The $PM_{2.5(Tr)}/PM_{10(Tr)}$ ratios range between about 0.67 and 1 for the background site and between

about 0.5 to 0.67 for the rural site. Whereas, the $PM_{1(Tr)}/PM_{10(Tr)}$ ratios are comparable for both sites from about 0.65 to 0.4.

As such, the ratios of tracers generally related to combustion sources can have comparable proportions in each PM size fraction. Hence, they can be grouped on the triangular diagram showing a characteristic signature.

The calculated ratios for tracers such as K , SO_4^{2-} , NH_4^+ and NO_3^- , attributed to more than one characteristic source, can be found in very different places on the triangular diagram. Results show that the calculated tracer ratios generally relate to combustion emissions, secondary aerosols and long-range transport such as SO_4^{2-} and NH_4^+ Makkonen et al. (2010), Lin et al. (2012) and Rogula-Kozłowska et al. (2013) are plotted on the left side of the triangular diagram. Here, the tracer concentrations of the fine and intermodal size fractions are predominant over the tracer concentrations of the coarse size fraction. The $PM_{2.5(Tr)}/PM_{10(Tr)}$ ratios are between 0.8 and 1, the $(PM_{2.5(Tr)}-PM_{1(Tr)})/(PM_{10(Tr)}-PM_{1(Tr)})$ ratios are between about 0.5 and 1, while $PM_{1(Tr)}/PM_{10(Tr)}$ ratios show a wide variation between about 0.2 and 0.9 (Fig.2). The $PM_{1(Tr)}/PM_{10(Tr)}$ ratios range from 0.8 to 0.9 for the Asian outflows site (Lim et al., 2012), from 0.7 to 0.8 for the urban background site (Rogula-Kozłowska et al., 2013) and from 0.5 to 0.7 or from 0.2 to 0.3 for a background site (Makkonen et al., 2010) depending on the season (See Fig.1). Moreover, sulphate and ammonium are comparable in proportion in each PM size fraction and show characteristic signatures. The calculated tracer ratios of NO_3^- which can also be related to secondary aerosols and long-range transport are not comparable in proportion to each PM size fraction with sulphate and ammonium reported for the Asian outflows site (Lim et al., 2012) and the background site (Makkonen et al., 2010). On these sites the $PM_{2.5(Tr)}/PM_{10(Tr)}$ ratios range between 0.4 and 0.5, the $PM_{1(Tr)}/PM_{10(Tr)}$ ratios range between about 0.05 and 0.3 and the $(PM_{2.5(Tr)}-PM_{1(Tr)})/(PM_{10(Tr)}-PM_{1(Tr)})$ ratios range between about 0.3 and 0.47. However, an exception exists for the background site reported by Rogula-Kozłowska et al. (2013) where the calculated ratios of SO_4^{2-} , NH_4^+ and NO_3^- are closely grouped (see Fig.2). This outcome can be explained by considering the reduced frequency of the combination SO_4^{2-} , NH_4^+ and NO_3^- (Viana et al., 2008).

Finally, the K tracer results highlight that it is associated to crustal sources in a background site (non-dust) (Matassoni et al., 2011) (see Fig.1) as well as to combustion sources in a background site (Makkonen et al., 2010) (see Fig.2). These results could be related to both city dust origin and biomass burning origin of the K tracer as reviewed by Viana et al. (2008).

4. Conclusions

The results highlight that tracers with the same ratios in each size fraction are closely displayed on the triangular diagram. These tracers, closely positioned, are related to the same sources, such as crustal matter, sea-salt, fuel-oil combustion, secondary aerosols and long-range transport. The triangular diagram reveals the characteristic signature of PM sources.

References

- Amato F., Pandolfi M., Escrig A., Querol X., Alastuey A., Pey J., Perez N., Hopke P.K. (2009). Quantifying road dust resuspension in urban environment by multilinear engine: a comparison with PMF2. Atmospheric Environment 43, 2770-2780.

- Belis C.A., Karagulian F., Larsen B.R., Hopke P.K. (2013). Critical review and meta-analysis of ambient particulate matter source apportionment using receptor models in Europe. *Atmospheric Environment* 69, 94-108.
- European Directive 2008/50/EC, Council Directive 2008/50/EC of the European Parliament and of the Council of 21 May 2008 on ambient air quality and cleaner air for Europe, <http://eur-lex.europa.eu/LexUriServ/LexUriServ.do?uri=OJ:L:2008:152:0001:0044:EN:PDF>
- Graham D.J., Midgley N.G. (2000). Graphical representation of particle shape using triangular diagrams: an Excel spreadsheet method. *Earth Surface Processes and Landforms* 25, 1473-1477.
- Lim S., Lee M., Lee G., Kim S., Yoon S., Kang K. (2012). Ionic and carbonaceous compositions of PM 10, PM 2.5 and PM 1.0 at Gosan ABC Superstation and their ratios as source signature. *Atmospheric Chemistry and Physics* 12, 2007-2024.
- Makkonen U., Hellén H., Anttila P., Ferm M. (2010). Size distribution and chemical composition of airborne particles in south-eastern Finland during different seasons and wildfire episodes in 2006. *Science of the Total Environment* 408, 644-651.
- Matassoni L., Pratesi G., Centioli D., Cadoni F., Lucarelli F., Nava S., Malesani P. (2011). Saharan dust contribution to PM 10, PM 2.5 and PM 1 in urban and suburban areas of Rome: a comparison between single-particle SEM-EDS analysis and whole-sample PIXE analysis. *Journal of Environmental Monitoring* 13, 732-742.
- Moreno T., Querol X., Alastuey A., Reche C., Cusack M., Amato F., Pandolfi M., Pey J., Richard A., Prévôt A.S.H., Furger M., Gibbons W. (2011). Variations in time and space of trace metal aerosol concentrations in urban areas and their surroundings. *Atmospheric Chemistry and Physics* 11, 9415-9430.
- Pope III C.A., Dockery D.W. (2006). Health effects of fine particulate air pollution: lines that connect. *Journal of the air & waste management association*, 56, 709-742.
- Rogula-Kozłowska W., Rogula-Kupiec P., Mathews B., Klejnowski K. (2013). Effects of road traffic on the ambient concentrations of three PM fractions and their main components in a large Upper Silesian city. *Annals of Warsaw University of Life Sciences-SGGW. Land Reclamation* 45, 243-253.
- Speranza A., Caggiano R., Margiotta S., Trippetta S. (2014). A novel approach to comparing simultaneous size-segregated particulate matter (PM) concentration ratios by means of a dedicated triangular diagram using the Agri Valley PM measurements as an example. *Natural Hazards and Earth System Science* 14, 2727-2733.
- Speranza A., Caggiano R., Margiotta S., Summa V., Trippetta S. (2016). A clustering approach based on triangular diagram to study the seasonal variability of simultaneous measurements of PM10, PM2.5 and PM1 mass concentration ratios. *Arabian Journal of Geosciences* 9, 1-8.
- Viana M., Kuhlbusch T.A.J., Querol X., Alastuey A., Harrison R.M., Hopke P.K., Winiwarter W., Vallius M., Szidat S., Prévôt A.S.H., Hueglin C., Bloemen H., Wählin P., Vecchi R., Miranda A.I., Kasper-Giebl A., Maenhaut W., Hitenberger R. (2008). Source apportionment of particulate matter in Europe: a review of methods and results. *Journal of Aerosol Science* 39, 827-849.
- Visser S., Slowik J.G., Furger M., Zotter P., Bukowiecki N., Dressler R., Flechsig U., Appert K., Green D.C., Tremper A.H., Young D.E., Williams P.I., Allan J.D., Herndon S.C., Williams L.R., Mohr C., Xu L., Ng N.L., Detournay A., Barlow J.F., Haliouk C.H., Fleming Z.L., Baltensperger U., Prévôt A.S.H. (2015). Kerb and urban increment of highly time-resolved trace elements in PM 10, PM 2.5 and PM 1.0 winter aerosol in London during ClearfLo 2012. *Atmospheric Chemistry and Physics* 15, 2367-2386.
- World Health Organization. Regional Office for Europe, & World Health Organization. (2006). Air quality guidelines: global update 2005: particulate matter, ozone, nitrogen dioxide, and sulfur dioxide. World Health Organization.